EXPERIMENTAL AND NUMERICAL STUDY OF THE PINCH DYNAMICS IN THE PF-1000 DEVICE

M. Scholz[1)], B. Bieńkowska[1)], I. Ivanova-Stanik[1)], A. Kasperczuk[1)], R. Miklaszewski[1)], M. Paduch[1)], T. Pisarczyk[1)], W. Stępniewski[1)], K. Tomaszewski[1)], P. Kubes[2)], J. Kravarik[2)]

1) Institute of Plasma Physics and Laser Microfusion, Hery 23, 00-908 Warsaw, P.O.Box 49, Poland;
[2)] Czech Technical University, Prague, Czech Republic

PACS: 52.58.Lq

1. INTRODUCTION

Plasma Focus devices belong to the family of the dynamic Z-pinch, where the dense and hot plasma is created. The plasma is formed by the discharge of a capacitor bank and the dynamics of the current sheet has two successive different phases: a long time scale phase (several microseconds) from breakdown to maximum compression during which the current sheet is formed and pushed by the Lorentz force; a short time phase (in the few tens of ns time scale) during which the pinch is created and disrupted by instabilities.

The fame of the PF has been based on the fact that it was the very intense neutron-producing device. The scaling laws for the neutron yields formulated at the beginning of the plasma focus investigations were very promising for these devices. Later investigations however carried out on bigger devices suggested that there is a certain condenser energy limit above which the scaling law is not valid. Hence the essential problem to be resolved in PF research has always been to discover the physics, which dominates the configuration, a question closely related to the neutron production mechanism and plasma dynamics.

In this paper, experimental and numerical investigations of last phase of plasma sheet dynamics in large scale PF are presented.

The physical model for numerical simulations is based on the set of non-ideal MHD equations in the two-fluid approximation with coupled equation of ionization kinetics. To study the evolution of the plasma an optical frame camera with exposure time of 1 ns were employed. On the basis of the plasma imager the dynamics of the plasma sheet evolution and plasma dimension were determined.

The experimental observations from large-scale PF-1000 machines are compared with numerical calculations of plasma evolution for parameters of PF-1000. Therefore, the main aim of the experiments was to determine operational regimes of the PF-1000 facility, in which the maximum neutron emission occurs, and to define characteristic features of the last phase of plasma evolution.

2. THE APPARATUS

The large scale PF-1000 facility consists of following main units:

- the condenser bank and pulsed electrical power circuit with a collector and low-inductance cables.
- the mechanical vacuum and gas system consist of the vacuum chamber, coaxial electrodes and gas handling system.

The electrical energy is transferred to a collector and electrodes by means of low-inductance cables. The vacuum chamber, which surrounds the electrodes, has a large volume (1400 mm in diameter and 2500 mm in length). Two coaxial electrodes are shown on Fig. 1. The outer electrode (cathode) consists of 24 stainless steel rods with 32 mm in diameter. The outer electrode (OE) and copper center electrode (CE) radii are 200 and 115.5 mm respectively with CE length of 600 mm. The cylindrical alumina insulator sits on the CE and the main part of the insulator extends 113 mm along the CE into the vacuum chamber. The insulator prescribes the shape of the initial current sheet between the CE and the back plate of the OE.

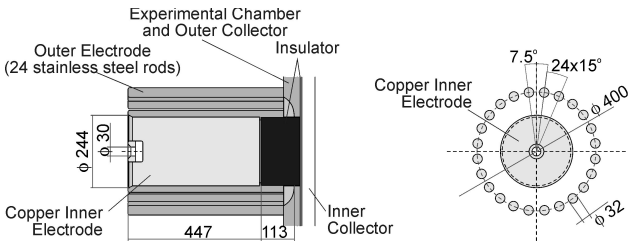

Fig. 1. Geometry of the electrodes of the PF-1000 device

The condenser bank of capacitance 1332 μF was charged to voltage ranging between 20-40 kV, which corresponded to discharge energies ranging from 266 kJ to 1064 kJ. During the described experiment the condenser bank was charged to 33 kV. The total energy stored in the bank was 725 kJ, while the maximum discharge current reached the value of 1.7 MA.

3. EXPERIMENTAL ARRANGEMENT

The scheme of the experimental set-up is shown on Fig. 1. To study the evolution of the plasma, a three frame optical camera with exposure time of about 1 ns was employed (see Fig. 2). In the case of the optical camera, image converters are used as a fast shutter and light amplifier. This camera allows capturing a frame plasma images with spatial resolution of 0.4 mm.

The delay between subsequent frames is in the range of 10 or 20 ns. An interference filter (λ_{max} = 593 nm, FWHM = 6 nm) was put into the optical path of the

passive optical diagnostic subsystem. Its spectral position enabled to record only continuous radiation.

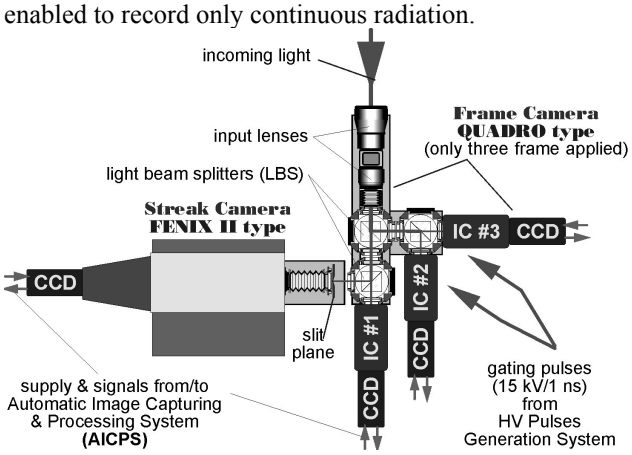

Fig. 2. Scheme of the passive optical system

In addition the following diagnostics were used:

- *dI*/*dt* probe for registration of the discharge current derivative (after performance of a numerical integral procedure). It was mounted inside of the PF-1000 collector;
- P-I-N diode for registration of the soft X-ray emission from the plasma column. This emission was observed by 230 μm pinhole in front of the diode. This diode was blocked by a 10 μm Be foil, therefore the diode sensitivity covered the range of 0.8 ÷ 10 keV;
- silver activation counters for estimation of the neutron yield; only the side-on counter reading was taken into account).

The soft X-ray signal detected by the P-I-N diode was used for synchronization purposes and determination of the temporal relation between the maximum compression of the plasma and frame images recorded by means of optical diagnostics. The special electrical and optical synchronization arrangement allowed synchronizing the optical diagnostics and the PF phenomenon with a temporary precision of 5 ns.

4. EXPERIMENTAL RESULTS

An investigation of the PF-1000 facility was carried out in the deuterium pressure range of 1 ÷ 5 Torr and a discharge energy level exceeding to 1 MJ. The obtained result have been successively published [1 – 4] and they can be summarized as follows:

1. PF-1000 facility can be operated with a regular and reproducible neutron emission (of the order of 10^{10} ÷ 10^{11} neutron/shot);
2. It was found that for each filling pressure value (p) neutron yield (Y_n) increases initially as a function of the charging voltage (V_0) up to maximum and after that it decreases with a further increase in V_0.
3. Two (or three) neutron pulses about 2 μs apart were observed in most of the discharges.

It is therefore of considerable importance to investigate the connection between the various mechanisms responsible for the neutron production and formation of PF radially collapsing sheet, the quality of the sheet velocity and the resulting pinch plasma as well as the stability and break-up of this pinch.

A sequence of frame camera pictures of discharges carried out in deuterium filling gas (p = 3 Torr), are shown on Fig. 3. The images were taken at different times during the implosion (Fig. 3a), minimum radius (Fig. 3b) and post pinch instability phase (Fig. 3c). The anode is on the left side of the pictures.

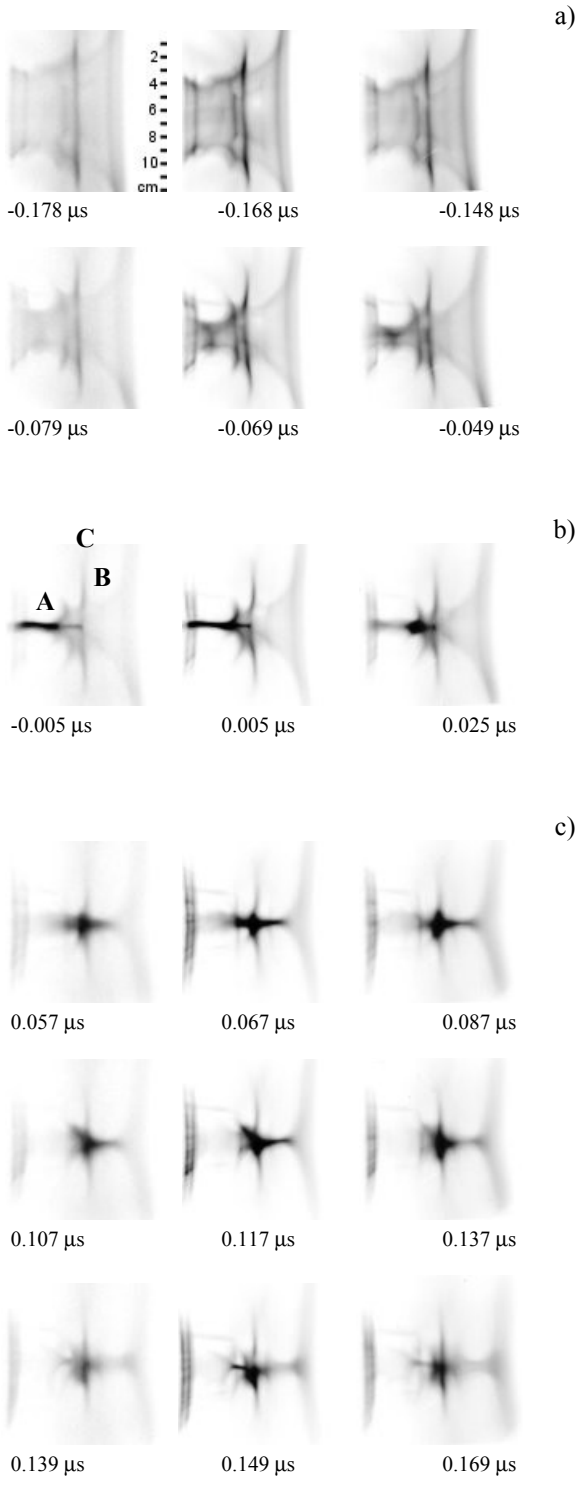

Fig. 3. A set of frame camera pictures of pinching dynamics (PF-1000 results in 2002: a) implosion phase; b) minimum radius phase; c) post pinch phase

In the images a strong surface of plasma sheet perturbations can be found. These surface perturbations could be traced back to that appearing early on in the sheet during the radial compression. This perturbation remains more or less frozen in until radial compression and tends not to destroy the integrity of the collapsing column. The upper part of the collapsing sheet has a low radial velocity of compression. These perturbations have a ring like shape around the surface of the plasma column as is shown in Fig. 3a. The trajectory of characteristics points (maximum or minimum) of the perturbations is approximately perpendicular to the axis of the electrodes.

The pinch column tends to develop into multiple necking as the pinch evolves. An example is shown in Fig. 3b. The necking develops at different z along the pinch column, each pushing plasma material away from the neck. The occurrence of two such regions would produce a jet like expansion of plasma at the junction between the two regions. This can be seen referring to the positions marked A, B and C on a picture on Fig. 3.

A and B mark the positions of the two collapsing and than necking regions while C clearly develops into a great scale perturbation. It has a clear border and an amplitude reaching size of 5 cm. This type of perturbation is stable and its lifetime is about 1 μs. The large-scale perturbation appears about 8 cm from the anode.

The period of the plasma column creation lasts about 200 ns. After this time a plasma column of about 12 cm in length should exist. So long time of plasma column creation results in a disruption of the earliest created part (see mark A) of the plasma column before the creation process of the whole pinch is finished. As a rule the minimum radius ($r_{\min}$) of plasma column in any cross section is 0.7 cm.

In the PF scheme one relies on the development of self-consistent phenomena occurring after maximum compression during the cylindrical re-expansion of the plasma column. Anomalous microscopic effect are probably responsible for particle heating while instabilities create a favorable situation for the onset of relaxation processes of the magnetized plasma, which lead to the formation of a sheet plasma configuration (the great plasma perturbations).

Its lifetime exceeds by an order of magnitude the transit time of reacting particles. In such a case the efficiency of energy transfer from the source of the magnetic energy stored in the system, as the distribution of current densities in the plasma column, are of paramount importance.

5. NUMERICAL MODEL

In order to address the questions of the sheet dynamics we developed a two-dimensional, two fluid, non-ideal MHD code. This code is based on the modified Dyachenko-Jach code [5], which includes kinetic of ionization. With this model it is possible to simulate the main features of the compression and expansion phase of the PF.

The magnetohydrodynamics equations in this code are described in detail elsewhere [6-8]. They are solved for six unknown variables namely the mass density ρ, The radial and axial moments ρ_{vr} and ρ_{vz}, the ion and electron temperatures T_c and T_e and the azimuthal magnetic field B_φ. All other quantities follow from these variables. Transport coefficients are given by Braginski, therefore we obtain the following system of equations:

$$\frac{d\rho}{dt} = -\rho\nabla\cdot\vec{u}$$

$$\rho\frac{du}{dt} = -\nabla p + \nabla\cdot\Pi + \frac{1}{c}\vec{j}\times\vec{B}$$

$$\rho c_{ve}\frac{dT_e}{dt} = -\nabla p_e\nabla\cdot\vec{u}_e - \nabla\cdot\vec{q}_e + \frac{1}{en_e}\vec{R}\cdot\vec{j} - Q_{e-i} - Q_{ioniz}$$

$$\rho c_{vi}\frac{dT_i}{dt} = -p_i\nabla\cdot\vec{u} + \Pi_i\cdot\nabla\vec{u} - \nabla\cdot\vec{q}_i + Q_{e-i}$$

$$\frac{dB}{dt} = \nabla\times\left[\vec{u}\times\vec{B} + \frac{c}{en_e}\left(\nabla p_e - \vec{R}\right) + \frac{1}{en_e}\vec{j}\times\vec{B}\right]$$

$$\vec{j} = \frac{c}{4\pi}\nabla\times\vec{B}$$

where:

$$\frac{d}{dt} \equiv \frac{\partial}{\partial t} + \vec{u}\cdot\nabla$$

$$u = \left(u_r, 0, u_z\right)$$

$$B = \left(0, B_\varphi, 0\right)$$

$$j = \left(j_r, 0, j_z\right)$$

$$p = p_e + p_i$$

$$\Pi = \Pi_i + \Pi_{\text{ort}}$$

$$\nu_e = \nu_{e-i} + \nu_{e-n}$$

$$\nu_i = \nu_{i-i} + \nu_{i-n}.$$

Most of these equations are self-explanatory. It should be noted that in the energy equations, the convective and advective terms contain the velocities of the species under consideration. Also anomalous resistivity caused by.

Apart from the ion velocity u, – or ambipolar – plasma velocity, we also need the electron velocity:

$$\vec{u}_e = \vec{u} - \frac{m_i j}{\rho e}.$$

In equation for electron temperature we included Joule heating, energy exchange with ions and ionization. Equation for ion temperature contains the exchange between ions and electrons.

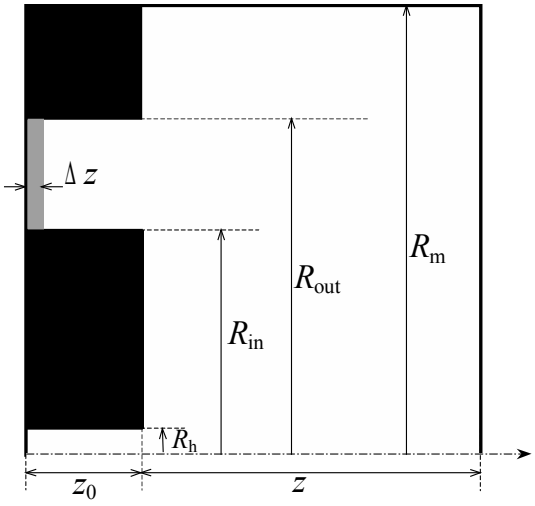

Fig. 4. Initial conditions of numerical calculations: R_{in} = 12 cm, R_{out} = 18 cm, R_h = 1.5 cm (hole radius), R_m = 24 cm, z = 18 cm, z_0 = 6 cm, Δz = 0.9 cm (current sheet thickness)

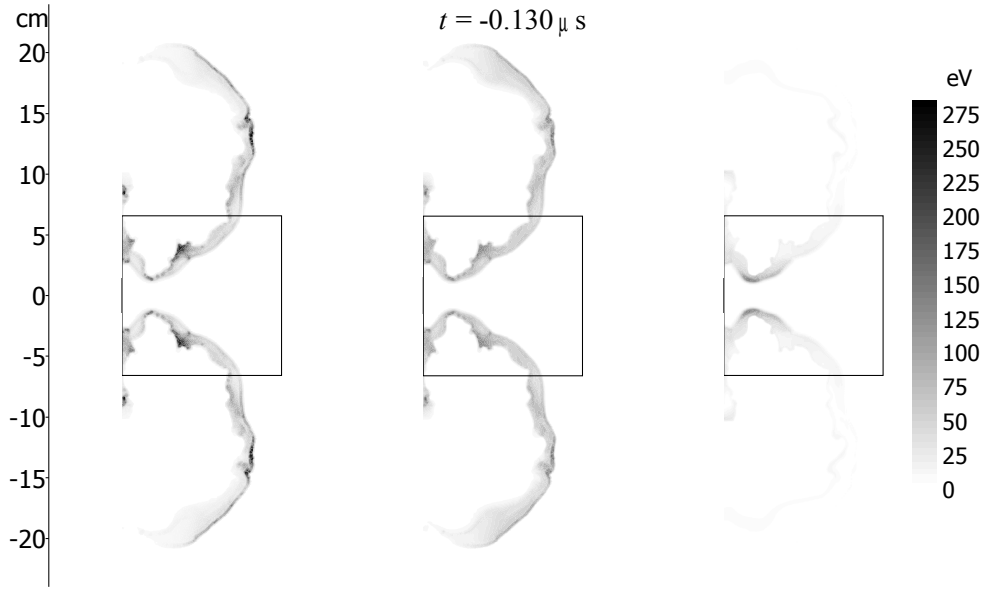

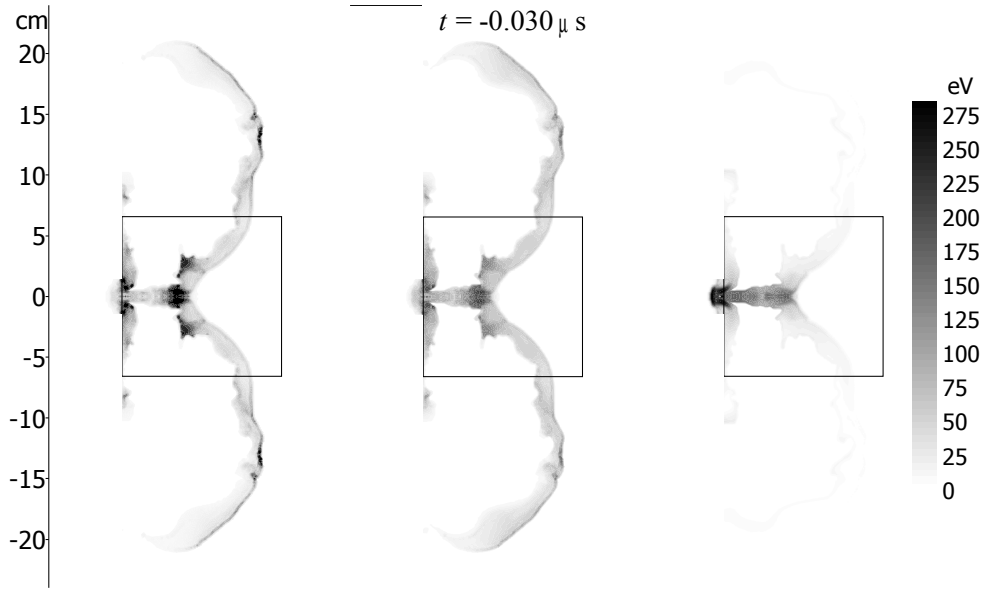

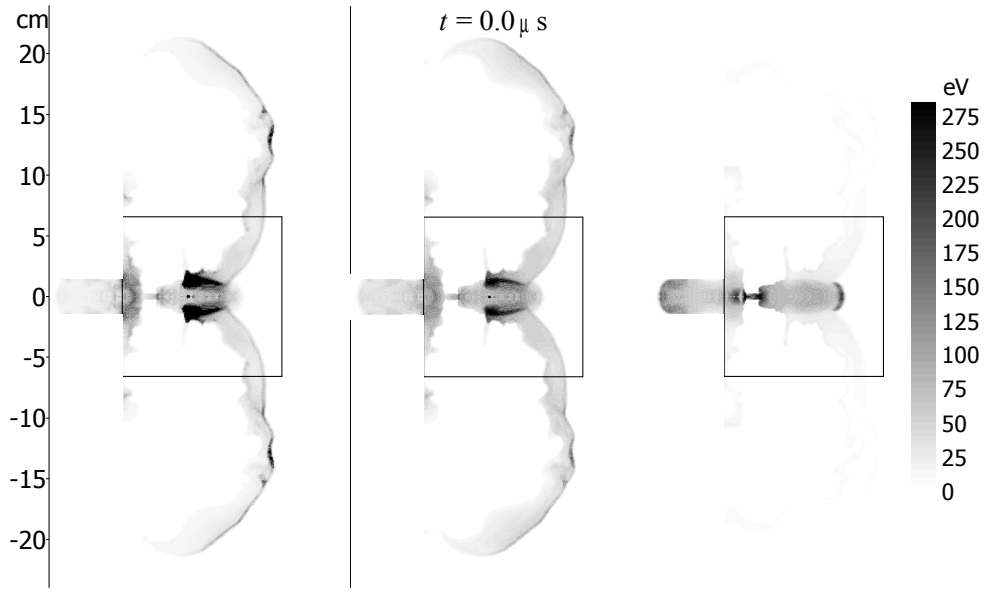

Fig. 5. A set of calculated spatial distributions of the plasma luminosity, particle density and ion temperature for three time steps

A different treatment is necessary for the inelastic processes. We consider electron impact ionization from the ground state radiative recombination and three body Auger recombination.

Since ionization and recombination are extremely strong functions of electron temperature and density respectively, it is not possible to solve the resulting equation:

$$\frac{dn_e}{dt} = n_e(n_0 - n_e)\cdot S - \alpha_r n_e^2 - \beta_{3B} n_e^3 .$$

within the algorithm for the MHD equations because numerical stability would require very small time step.

There were boundary conditions of a typical nature:

- on the pinch surface:

$$n \cdot q_i = 0 , \quad \vec{n} \cdot q_e = 0 ,$$
$$B|_{r=r_p} = \frac{2I}{cr_p} ,$$
$$n \cdot (\vec{\vec{p}}I - \vec{\vec{n}}) = 0 ,$$

- on the electrode:

$$u_n = 0 ,$$
$$\frac{\partial T_e}{\partial n} = 0 , \quad \frac{\partial T_i}{\partial n} = 0 ,$$

- on the axis:

$$u_r = 0 ,$$
$$B_\varphi = 0 ,$$
$$\frac{\partial T_e}{\partial r} = 0 , \quad \frac{\partial T_i}{\partial r} = 0 .$$

We have started the two-fluid calculations with formed current sheet, which parameters were as follows: the current sheet thickness Δz = 0.9 cm, the temperature is assumed to be 5 eV. The current sheet has started 6 cm before the end of the electrodes (Fig4). The initial current through the sheet was chosen (from experiment) equal to 1.7 MA. Subsequently, the current is determined by the magnetic flux conservation:

$$L \cdot I = \text{const} .$$

The filling pressure D_2 was 3 Torr with 0.1% homogeneously ionized deuterium plasma and initial temperature of the deuterium plasma was equal to 0.5 eV.

Fig. 5 shows the calculated spatial distributions of the plasma luminosity, density and ion temperature for three time steps. The square marked on the pictures is the area observed by the frame camera in our experiment.

Our calculations clearly show the instabilities that take place in a plasma focus device and give qualitative information about their temporal evolution (see Fig. 5). The appearance of RT instabilities on the plasma sheet is detected during the radial collapse phase. These perturbations do not grow significantly during the radial compression stage and they are apparently frozen in the plasma sheet. The initial perturbations on the plasma sheet lead to the growth of strong perturbations at pinch time. Multiple necking is observed on the much tightly pinched dense plasma column. This is in line with the frame camera observations on PF-1000 device.

6. CONCLUSIONS

1. Preliminary results agree qualitatively and quantitatively with experimental results.
2. The velocity computed for the run down phase is lower than the measured one: $v_{z\ \mathrm{exp}} = 8 \cdot 10^6$ cm/s; $v_{z\ \mathrm{com}} = 6.8 \cdot 10^6$ cm/s.
3. Qualitative agreement of experimentally observed pinch dynamics and structures with numerical modeling of the pinch phase.
4. Specific features of PF-1000 phenomena: independent radial dynamics in separate two or three pinches positioned one after another along the axis.
5. Stable plasma radiating structures on axis situated in-between of two pinching sequences of a pinch.

REFERENCES

[1] M. Scholz, L. Karpinski, M. Paduch et al./ *Proc. 27th IEEE Int. Conf. Plasma Science, COPS 2000, New Orelan, USA*. 1C 09:94.

[2] M. Scholz, L. Karpinski, M. Paduch et al.// *Nukleonika.* (46). (supplement), 2001, p.35.

[3] A. Szydlowski, M. Scholz, M. Paduch et al.// *Nukleonika.* (46). (supplement), 2001,p. 61.

[4] M. Scholz, R. Miklaszewski, M. Paduch et al.// *IEEE Trans on Plasma Science* (30). 2002, p.476.

[5] K. Jach et al.// *Comput. Assisted Mech. Eng. Sci*. (2), 1995, p.2.

[6] D. E. Potter// *Phys. Fluids* (21), 1971, p. 1911

[7] V. P. Dyachenko, V. S. Imshennik// *Sov. Phys. JETP* (29), 1969, p.947.

[8] S. Maxon, J. Eddleman// *Phys. Fluids* (21). 1978, p.1856.